Science of the Total Environment 771 (2021) 145410

Contents lists available at ScienceDirect

Science of the Total Environment

journal homepage: www.elsevier.com/locate/scitotenv

Evaluation of microwave soil moisture data for monitoring live fuel moisture content (LFMC) over the coterminous United States

Yang Lu [a], Chunzhu Wei [b,c,*]

[a] Geography and Environment, University of Southampton, Southampton, United Kingdom
[b] School of Geography and Planning, Sun Yat-sen University, Guangzhou, China
[c] Southern Marine Science and Engineering Guangdong Laboratory (Zhuhai), Zhuhai, China

HIGHLIGHTS

- ESA ECV SM and LFMC relationship was evaluated over the coterminous US.
- Major fuel types with a high response to soil moisture were determined.
- Soil moisture has a higher correlation with LFMC under dry conditions.
- Utilities of surface and root-zone soil moisture are comparable.

GRAPHICAL ABSTRACT

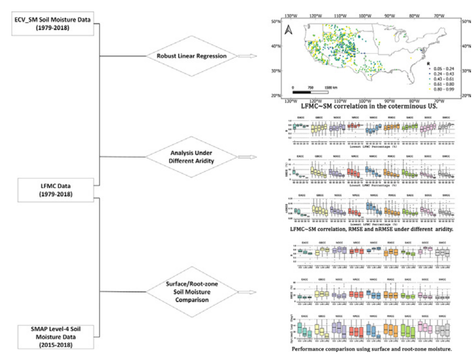

ARTICLE INFO

Article history:
Received 20 September 2020
Received in revised form 16 January 2021
Accepted 21 January 2021
Available online 29 January 2021

Editor: Paulo Pereira

Keywords:
Live fuel moisture content
Soil moisture
Microwave
ESA ECV SM
SMAP Level-4

ABSTRACT

Live fuel moisture content (LFMC), which is the ratio of water in the fresh biomass to the dry biomass, is a key variable that affects wildfire behaviour. Previous studies have assessed soil moisture as a predictor of LFMC over small areas with limited data, but a comprehensive evaluation at sub-continental scale is still lacking, and the explanatory utility has not been evaluated under different aridity conditions. In this study, the utility was evaluated using microwave soil moisture data from the ESA ECV_SM product from 1979 to 2018 and LFMC data from over 1000 sites in the coterminous United States. A time-lagged robust linear regression model was adopted, and the results were compared with analysis from in situ soil moisture measurements at adjacent sites. The results suggested that at most sites the LFMC correlates best with soil moisture within 60 days prior to LFMC sampling, and that the correlation is lower in areas with complex terrain. LFMC can be estimated from soil moisture with a mean RMSE of around 20%. The correlation between LFMC and soil moisture is significant ($p<0.01$) in most regions, and is mostly stable in different years. The major fuel types with a high response to soil moisture include pine, redcedar, sagebrush, oak, manzanita, chamise, mesquite and juniper, depending on the region. The LFMC ~ soil moisture correlation varies with the aridity condition, and soil moisture has a higher explanatory utility on LFMC under dry conditions. An analysis using SMAP Level-4 product indicated that the surface and root-zone soil moisture perform similarly in LFMC estimation. This study suggests that microwave soil moisture data contain sufficient information on LFMC, and may serve as a reference for the development of more sophisticated LFMC estimation methods.

* Corresponding author at: School of Geography and Planning, Sun Yat-sen University, Guangzhou, China.
E-mail address: weichzh@mail.sysu.edu.cn (C. Wei).

https://doi.org/10.1016/j.scitotenv.2021.145410
0048-9697/

1. Introduction

Wildfire burns over 4 million km^2 of land area per year globally (Giglio et al., 2018), and has shown an increasing trend of occurrence (Dennison et al., 2014; Donovan et al., 2017) as well as prolonged fire season under the changing climate (Liu et al., 2010; Jolly et al., 2015). As a key variable that affects wildfire ignition, spread and severity (Chuvieco et al., 2002; Rossa et al., 2016; Rossa, 2017; Ruffault et al., 2018; Kelley et al., 2019), the live fuel moisture content (LFMC), which is the ratio of the water contained in the fresh biomass to the dry biomass, has long been used as an indicator to assess wildfire risk (Deeming, 1972; Stocks et al., 1989; Weise et al., 1998; Jolly, 2007). LFMC can be measured using field sampling and gravimetric method (Countryman and Dean, 1979), and is routinely monitored by a number of regional and national networks. This method is locally accurate and provides a reliable point-scale reference. However, the field sampling and oven-drying processes are costly and labor-intensive (Yebra et al., 2013). More importantly, the extrapolation from the point measurements to regional scale or a longer period is problematic (Fan et al., 2018), particularly in areas with heterogeneous landscape or various plant species (Yebra et al., 2013; Ruffault et al., 2018; Jolly and Johnson, 2018; Karavani et al., 2018; Rao et al., 2020).

To obtain spatially distributed and temporally consistent LFMC estimates, various methods have been developed to derive LFMC estimates from remote sensing data, which can be broadly classified into physically-based and empirical methods. The physically-based models build on the radiation absorption effect of tissue water content, which reduces the spectral reflectance in the solar radiation domain (Yebra et al., 2013). However, the LFMC dynamics are also affected by the pigment and chlorophyll concentration as well as the internal leaf structure, and applications call for extensive calibration and validation (Fan et al., 2018). In addition, the mechanism of LFMC dynamics involves its interactions with the atmosphere and plant physiological processes, which are still poorly understood (Jolly et al., 2014; Ruffault et al., 2018). The empirical methods aim to statistically fit a relationship between LFMC and other predictors derived from remote sensing. Commonly used predictors include those that quantify the aridity condition (Keetch and Byram, 1968; Van Wagner et al., 1987; Dimitrakopoulos and Bemmerzouk, 2003; García et al., 2008; Ruffault et al., 2018) and those that depict the state of the canopy (Gao, 1996; Ceccato et al., 2002; Danson and Bowyer, 2004; Dennison et al., 2005; Peterson et al., 2008; Yebra et al., 2008; Myoung et al., 2018).

Among the predictors, soil moisture in particular has a direct influence on vegetation water content (Qi et al., 2012; Yebra et al., 2013; Fares et al., 2017). Previous studies have assessed the capacity of indices that contain soil moisture information, such as the Keetch Byram Drought Index (Keetch and Byram, 1968) and the Cumulative Water Balance Index (Dennison et al., 2003), and suggested that soil moisture deficit affects plant water potential, which determines the relative water content in the plant tissue (Wang et al., 2007; Qi et al., 2012; Fan et al., 2015). In addition, soil moisture can be measured using microwave sensors, which enable all-weather observations at relatively short intervals (typically 2–3 days). This makes soil moisture more advantageous than other indices based on optical or near-infrared measurements that are often susceptible to cloud contamination. Many microwave soil moisture products have been available in the past decades, such as the Advanced Microwave Scanning Radiometer (AMSR-E) (Njoku et al., 2003), the Soil Moisture and Ocean Salinity (SMOS) (Kerr et al., 2001), the METOP-A Advanced Scatterometer (ASCAT) (Bartalis et al., 2007), the Soil Moisture Active Passive (SMAP) (Entekhabi et al., 2010) and Sentinel-1 (Torres et al., 2012), among others. By merging soil moisture data from different microwave sensors, the Essential Climate Variables for Soil Moisture product (ECV_SM) was derived within ESA's Climate Change Initiative (CCI) (Dorigo et al., 2015; Gruber et al., 2019), which provides consistent global soil moisture data from 1978 at daily scale. Validation studies have revealed a good performance of the products (Dorigo et al., 2015; Colliander et al., 2017). In addition, microwave observations have also been used to derive root-zone soil moisture, either through recursive filtering (Albergel et al., 2008; de Jeu and Dorigo, 2016) or land surface data assimilation (Reichle et al., 2017a, 2017b). As root-zone soil moisture represents the moisture reservoir that can be directly utilized by the plant, it may be more informative on LFMC than the surface soil moisture (González-Zamora et al., 2016).

Recently, a few studies have evaluated the utility of microwave soil moisture data for LFMC estimation in southern California (Jia et al., 2019) and around the Mediterranean (Fan et al., 2018), but some limitations are still yet to be addressed. First, these studies were based on a limited number (<20) of LFMC sites and/or a short time period, and the results were usually not evaluated against in situ soil moisture data, which hinders the generalization of the findings. So far no such studies at sub-continental scale have been performed. Second, the plant species and the environmental conditions were often similar in a small study area, which essentially neglects the potential impact of vegetation type and environmental variability. Furthermore, previous studies predominantly evaluated a constant relationship between LFMC and soil moisture regardless of the aridity condition, which was based on an implicit assumption of a uniform response of LFMC to soil moisture under different soil wetness conditions. In fact, vegetation may respond to soil moisture at different intensities under different aridity conditions, which has not been addressed in previous studies. As wildfire is usually related to low LFMC values, the LFMC ~ soil moisture relationship under dry conditions would be more informative on wildfire risk assessment.

In this study, a comprehensive analysis is performed for the conterminous United States using data from over 1000 LFMC sites between 1979 and 2018. This is the first study that addresses LFMC and soil moisture correlation at this scale, and it significantly exceeds previous studies in the sample size, study period and comprehensiveness. This study aims to answer the following questions: (i) What is the utility of microwave soil moisture for estimating LFMC in different regions of the coterminous United States? (ii) What are the vegetation types whose LFMC are most sensitive to soil moisture? (iii) Is there a difference in the LFMC ~ soil moisture relationship under different aridity conditions? (iv) Does root-zone soil moisture have added value on LFMC estimation compared to surface soil moisture? The main objectives were to evaluate the utility of microwave soil moisture data for LFMC estimation, which would benefit the development of more sophisticated LFMC prediction models.

2. Materials and methods

2.1. LFMC data

The LFMC data used in this study were acquired from the National Fuel Moisture Database (NFMD). The NFMD is a web-based query system that is maintained by the United States Forest Service and is primarily administered at Geographic Area Coordination Center (GACC) level. There have been 1064 LFMC sites administered by nine GACCs in the coterminous United States (shown in Fig. 1 and Table 1), covering a record length from a couple of years to over 30 years. The sites are predominantly located in the western United States, which features frequent wildfire events (Westerling et al., 2006; Dennison et al., 2014). A total of 238,294 fuel moisture samplings were analyzed in this study. The sampling covers a wide range of live fuel types representative to the region, such as pine, sagebrush, juniper, chamise, fir and oak, among others. The field sampling is typically conducted bi-weekly during summer and autumn (Qi et al., 2012) during dry days free from dew or precipitation. The fresh mass is weighed in the field, and the dry mass is weighed after at least 24 h drying at 100 °C. Many sampling sites feature multiple species and/or dead fuels (dead twigs and leaves, fallen branches, litter or other dead organic materials). At these site, both

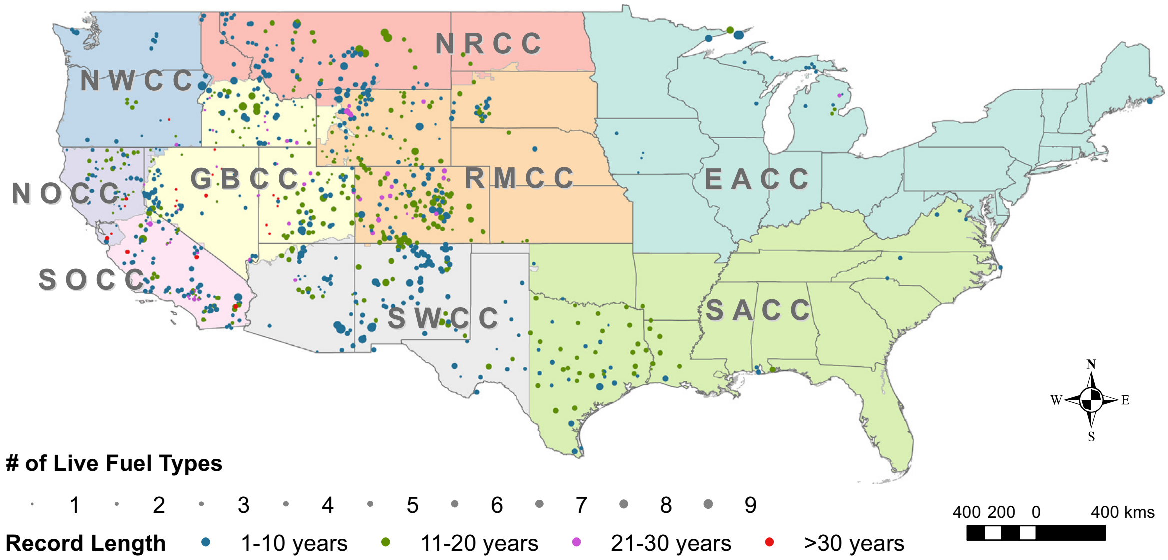

Fig. 1. LFMC sampling sites from the National Fuel Moisture Database (NFMD). The GACC acronyms are listed in Table 1.

dead fuel moisture content (if any, up to 5 dead fuel types) and the LFMC of up to 9 live fuel types are recorded. The LFMC value is calculated by

$$LFMC = \frac{m_f - m_d}{m_d} \times 100\% \quad (1)$$

where m_f and m_d are the fresh and dry mass weights of the vegetation samples.

2.2. In situ soil moisture data

The in situ soil moisture observations from the Soil Climate Analysis Network (SCAN, Schaefer et al. (2007)) were used to evaluate the performance and representativeness of the ECV_SM product for estimating LFMC at point scale. SCAN consists of 225 soil moisture sites, and only those located nearby a LFMC sampling site (within 0.1° in this study) were selected. At SCAN sites, soil moisture data are routinely measured hourly at the depths of 5, 10, 20, 50 and 100 cm below the surface. To be consistent with the penetration depth of ECV_SM data, SCAN data at 5-cm depth were used for the evaluation.

2.3. Remote sensing soil moisture data

Two soil moisture products based on microwave remote sensing were used, namely the ESA ECV_SM product and the SMAP Level-4 product. The ESA ECV_SM provides a long record (since 1978) of global surface soil moisture data, and is used to evaluate the relationship between surface soil moisture and LFMC. The SMAP Level-4 product is based on land surface data assimilation and provides global surface and root-zone soil moisture data, and is used to assess the utility of surface and root-zone soil moisture in estimating LFMC.

The ESA ECV_SM products are generated by harmonizing and merging soil moisture retrievals from multiple satellite sensors into a consistent and quality-controlled long-record global soil moisture data set (Gruber et al., 2019). This data set incorporates soil moisture products retrieved from both passive and active microwave remote sensing at L-band (1–2 GHz), C-band (4–8 GHz) and even higher frequency (Gruber et al., 2019). The soil penetration capacity decreases with higher frequency and denser vegetation. The nominal soil penetration depth is around 5 cm at L-band (Entekhabi et al., 2010), and around 2–3 cm at C-band (Brocca et al., 2016). Three daily soil moisture products were provided on 0.25° grids: (i) the active-microwave-based product, (ii) the passive-microwave-based product, and (iii) the combined active-passive product. Here the combined active-passive product (v04.4) from January 1, 1979 to June 30, 2018 was adopted to maximize data availability.

The SMAP Level-4 soil moisture is a value-added product generated by assimilating the SMAP L-band brightness temperature observations into the Catchment Land Surface Model (CLSM) (Reichle et al., 2017b). Both soil moisture data of the surface (0–5 cm) and root-zone (0–100 cm) are provided globally on 9-km Equal Area Scalable Earth-2 (EASE2) grids every 3 h from March 31, 2015. Validation studies have suggested a good performance in characterizing soil moisture dynamics at the surface and the root-zone, especially in the United States (Reichle et al., 2017a). In this study the SMAP Level-4 surface and root-zone soil moisture data (v4) from March 31, 2015 to June 30, 2018 were used.

Table 1
Information on the nine Geographic Area Coordination Centers (GACCs). The site-mean soil moisture is calculated using ECV_SM data.

GACC	Sites	Site-mean SM	Mean record (year)	Mean # of live fuel types	# of records
Eastern Coordination Center (EACC)	32	0.26	5.3	2.5	7343
Great Basin Coordination Center (GBCC)	207	0.16	14.2	2.4	61,386
Northern California Coordination Center (NOCC)	120	0.17	10.2	1.9	16,380
Northern Rockies Coordination Center (NRCC)	99	0.20	6.6	3.2	14,329
Northwest Coordination Center (NWCC)	39	0.19	9.2	2.2	4973
Rocky Mountain Coordination Center (RMCC)	220	0.18	11.9	2.6	58,985
Southern Coordination Center (SACC)	87	0.24	9.5	3.1	17,693
Southern California Coordination Center (SOCC)	130	0.13	12.8	2.1	35,795
Southwest Coordination Center (SWCC)	130	0.16	7.2	3.3	21,410

2.4. Methodology

2.4.1. Time-lagged robust linear regression

When the soil surface is wetted after a precipitation event, it takes some time for the water to infiltrate into the root-zone and be utilized by the plant. Likewise, during a dry spell the soil profile dries down gradually from the surface to the deeper layers. Consequently, the surface soil moisture condition on the day of LFMC sampling does not have an immediate impact on the vegetation condition (Jia et al., 2019). In contrast, the soil moisture measured several days (weeks) before LFMC sampling may be more informative on the LFMC values as the soil water has infiltrated into the deeper soil and can be utilized by the plant roots. Here a time-lagged correlation analysis was used to evaluate the utility of soil moisture data to estimate LFMC. Different from some previous studies which have used ordinary linear regression (Fan et al., 2018; Jia et al., 2019), a correlation analysis based on the robust linear regression is adopted. The ordinary regression normally works well when the underlying assumptions are true, but may give misleading results when the assumptions are violated. As an alternative to ordinary regression, robust regression works by assigning a weight iteratively to each data point. All data points are given uniform weights in the initial iteration, and regression coefficients are estimated using ordinary regression. In the subsequent iterations, weights are recomputed so that data points further away from model predictions are given lower weights, and the corresponding regression coefficients are updated. The iteration continues until the regression coefficients converge within a given tolerance. This way the impact of outliers on the evaluation is reduced, which can be significant at some sites using the ordinary least-square regressions.

The bisquare weights method is used to minimize the weighted sum of error estimate

$$S=\sum_{i=1}^{n} w_i (y_i - \hat{y}_i)^2 \tag{2}$$

where S is the weighted square error, n is the number of data points, w_i, y_i and $\hat{y}_i$ are the weight, observation and model prediction of data point i. The standardized adjusted residual is given by

$$u_i = \frac{r_i}{Ks\sqrt{1-h_i}} \tag{3}$$

where is the usual least-squares residual, h_i is the leverage that adjusts the residuals by reducing the weight of high-leverage data points. K is a tuning constant equal to 4.685, and s is the robust standard deviation given by $MAD/0.6745$ where MAD is the median absolute deviation of the residuals.

The weights are calculated by

$$w_i = \begin{matrix} (1-u_i^2)^2 & |u_i| < 1 \\ 0 & |u_i| \geq 1 \end{matrix} \tag{4}$$

The weights are calculated iteratively until the fit converges.

2.4.2. LFMC response to soil moisture under different aridity conditions

Soil moisture and LFMC generally exhibit a positive correlation (i.e., higher soil moisture corresponds to a higher LFMC value). However, when soil moisture surpasses a certain threshold (e.g., near field capacity), further increasing soil moisture may have no or only marginal influence on LFMC as the plant is not water-stressed. If water logging is present after a large precipitation event, the high soil moisture may hinder plant respiration, which may even lead to reduced LFMC values. In contrast, if soil moisture drops to below permanent wilting point, the plant would start to wither, and would have no response to further soil moisture variations. In addition, the relationship of soil moisture and water stress is usually non-linear as a result of acclimation and adaptation to stress (Steduto et al., 2009). These all suggest that the LFMC may respond differently to soil moisture under different aridity conditions. In this study, the LFMC ~ soil moisture correlation was also analyzed for the lowest (i.e., driest) 50%, 40%, 30%, 20% and 10% of LFMC data separately at each site, and the results were compared to those using all LFMC data.

2.5. Experiment set-up

The LFMC data between January 1, 1979 and June 30, 2018 were first quality-controlled to remove dead fuel samplings and invalid records. The optimal time lag is then determined for each sampling site using the time-lagged robust linear regression, respectively. The time lag is expected to be site-specific, depending on the vegetation type, climate and local terrain. Previous studies have used a uniform time lag between 15 days to 2 months at different study areas (Fan et al., 2018; Jia et al., 2019). To determine the optimal time lag, the correlation coefficients between LFMC and the soil moisture data using different time lags were calculated within a pre-defined lag threshold, and the time lag that leads to the highest correlation coefficient was chosen as the optimum. Here the lag threshold was determined by calculating the maximum correlation coefficient that can be achieved within a lag threshold that gradually increases from 10 to 100 days with a 10-day increment. Once the threshold was determined, the optimal time lag was calculated for each LFMC site within the threshold. The analysis was done separately using ESA ECV_SM and SMAP Level-4 soil moisture products. To reduce the uncertainties caused by a small sample size, an arbitrary threshold of at least 10 LFMC ~ soil moisture data pairs was implemented in all the analyses. The analysis was performed using Matlab R2018a, and correlation with $p<0.05$ is considered statistically significant.

3. Results

3.1. Time lag threshold determination

The maximum correlation coefficients achieved within a maximum lag threshold of 10 to 100 days for each GACC are shown in Fig. 2. Here the correlation coefficients for all fuel types at each site are included. The improvement in the correlation coefficient is most evident when the maximum lag threshold increases from 10 days to 30 days, particularly in EACC and NOCC. When the threshold keeps increasing to 60 days, the improvement in the correlation coefficient is seen mostly in EACC and SOCC at a slower rate, while the improvement in other GACCs is less evident. When a threshold larger than 60 days is used, only marginal improvement is achieved at all GACCs. Based on the analysis, a maximum time lag threshold of 60 days was used in this study.

3.2. LFMC ~ ECV_SM correlation in the coterminous United States

Using a time lag threshold of 60 days, the maximum correlation coefficient and the corresponding optimal lag were calculated for each site (shown in Fig. 3). Different from Fig. 2 which includes all fuel types at each site, here only the fuel type with the highest correlation coefficient at each site is included in the analysis (i.e., one fuel type per site). This is to distinguish between the high-response and low-response vegetation to soil water content and to highlight the fuel types of which the LFMC is most predictable by soil moisture information. After quality control, 805 LFMC sites were analyzed in the coterminous United States. The median value in each GACC falls between 0.64 and 0.74, and the national average correlation coefficient is 0.66. Similar to the results shown in Fig. 2, the average correlation coefficient is the highest in NOCC and the lowest in SWCC. By comparing the correlation coefficients in Figs. 2 and 3, large differences are seen in SACC, SWCC, RMCC and NRCC. For example, the median value increases from 0.57 to 0.71 in SACC, from 0.54 to 0.66 in SWCC, from 0.54 to 0.64 in RMCC, and from

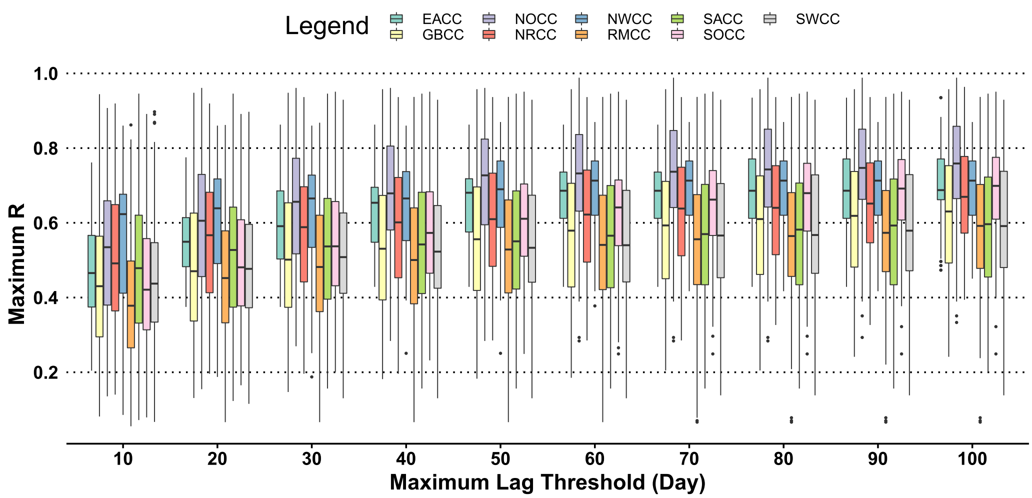

Fig. 2. Box plot of the correlation coefficients between LFMC and ESA ECV_SM data in the nine GACCs (represented by different boxes) with increasing maximum time lag threshold. The upper/lower boundary of the box and the whisker indicate the upper/lower quartile and the median values, respectively. The dots indicate outliers. The GACC acronyms are listed in Table 1.

0.62 to 0.71 in NRCC. While in other regions such as NWCC and NOCC, the median value only increases marginally by less than 0.01. The optimal lags determined generally feature a wide range from less than 10 days to over 50 days in all GACCs.

The correlation coefficients and LFMC estimation RMSE are shown in Fig. 4. In most GACCs, the estimation RMSE ranges between 0 and 40% with a GACC-average of around 20%. The estimates are mostly significant (p<0.01), and few sites yield a correlation coefficient lower than 0.4. However, at some sites in GBCC and RMCC, the estimation RMSE can be larger than 40%, and the lowest correlation coefficient can be smaller than 0.4. In these two regions, most of the sites are located in the Rocky mountain regions (Fig. 1), which feature complex terrain. In areas where the terrain is more uniform such as EACC and SACC, the soil moisture demonstrates a higher correlation with LFMC, and RMSE is significantly smaller than in regions with complex terrain.

The statistical metrics of fuel types with a high response to soil moisture variation in each GACC are listed in Table 2. Several fuel types have high responses to soil moisture in multiple GACCs, such as pine, sagebrush, oak and chamise. The mean correlation coefficients of the same vegetation are in general comparable among different GACCs, but the mean lag may differ considerable (e.g., for pine), which may be affected by the local climate and terrain. Among the high-response fuel types, pine LFMC is most predictable by soil moisture with a mean RMSE of 12.7%, followed by oak LFMC with a mean RMSE of 17.0%. In contrast, the mean LFMC estimation RMSE of sagebrush is 31.8%, despite the higher correlation coefficient.

The spatial patterns of the correlation coefficients and optimal lags are shown in Fig. 5. The distribution of correlation coefficients is relatively even, and no evident spatial agglomeration is seen. In southeast GBCC and western RMCC where the Rocky mountain is located, the correlation coefficients are relatively smaller than the surrounding areas, which is consistent with patterns shown in Fig. 4. The time lag pattern is affected by factors such as climate, local terrain and plant type, and is therefore more difficult to interpret. The time lag in SOCC is the highest among the GACCs (also shown in Fig. 3).

3.3. Comparison with LFMC ~ in situ soil moisture analysis

The LFMC data are sampled at point scale, while the ECV_SM product is based on satellite measurement with a much larger footprint than in situ measurements, which essentially smooths the soil moisture spatial variability within the grid cell to obtain the mean soil wetness condition. Therefore an implicit assumption is that the LFMC ~ ECV_SM analysis can well represent the results that would be derived

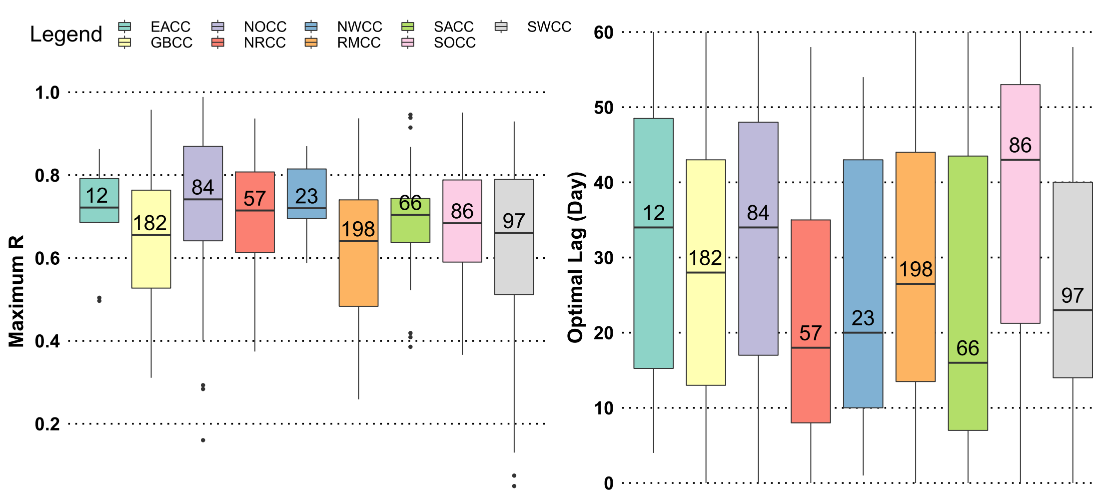

Fig. 3. Box plot of the maximum correlation coefficients and the optimal time lags at LFMC sites in the nine GACCs (represented by different boxes) using a time lag threshold of 60 days. The upper/lower boundary of the box and the whisker indicate the upper/lower quartile and the median values, respectively. The dots indicate outliers. The numbers above the whiskers indicate number of sites in the analysis. The GACC acronyms are listed in Table 1.

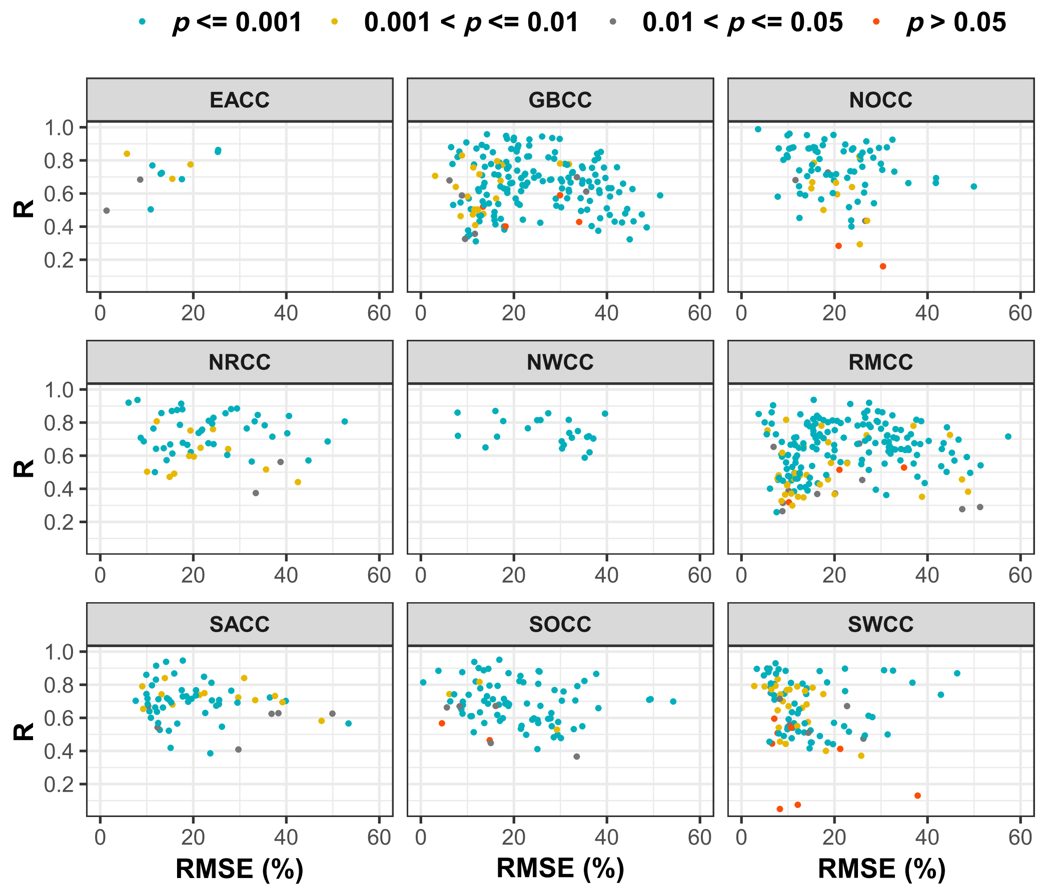

Fig. 4. The LFMC ~ ECV_SM correlation coefficient and LFMC estimation RMSE in different GACCs. The colors indicate different significance levels. The GACC acronyms are listed in Table 1.

if in situ soil moisture data were used. To evaluate the representativeness of ECV_SM data, it would be ideal to use in situ soil moisture data from the LFMC sampling site, which is usually unavailable. Here the LFMC ~ ECV_SM correlation coefficients and RMSEs are compared to the results derived using soil moisture data from nearby SCAN sites within a certain distance. A 0.1° distance threshold (≈9 km) was adopted, and 9 SCAN sites were found within the distance threshold of a NFMD site. The 9 NFMD sites are located in SOCC, NOCC, SACC and EGBC (3,1,2 and 3 sites, respectively) with 18 live fuel types in total. After quality control, the LFMC ~ SCAN soil moisture correlation was derived for 14 fuel types at 7 sites, and the results were compared with the LFMC ~ ECV_SM estimates. Here the possible difference between the SCAN measurement depth (5 cm) and the microwave penetration depth is not accounted for, and it is expected that the surface soil moisture temporal dynamics is similar within the several centimeters depth.

Table 2
Fuel types with a high response to soil moisture in each GACC. The GACC acronyms are listed in Table 1.

GACC	Fuel type	R mean	RMSE mean (%)	Lag mean (day)
EACC	Pine	0.67	12.9	36.2
	Redcedar	0.73	11.2	33.3
GBCC	Sagebrush	0.67	32.4	31.2
	Oak	0.69	19.0	15.9
NOCC	Manzanita	0.63	20.6	33.2
	Chamise	0.81	17.1	37.7
NRCC	Sagebrush	0.76	31.5	29.6
	Pine	0.65	14.5	13.3
NWCC	Sagebrush	0.74	31.1	20.8
RMCC	Sagebrush	0.67	32.0	32.8
	Oak	0.72	17.2	20.7
SACC	Oak	0.69	12.5	26.7
	Mesquite	0.70	24.4	21.7
SOCC	Chamise	0.68	19.3	37.8
	Manzanita	0.62	16.6	29.8
SWCC	Pine	0.65	10.8	29.6
	Juniper	0.63	11.2	21.0
	Oak	0.65	19.1	27.7

The comparison is shown in Fig. 6, and the robust regression method is also compared to the ordinary regression method. For most fuel types (excluding the outlier), the correlation coefficients obtained using ECV_SM or SCAN data agree very well ($r = 0.781$, $p = 0.001$), and the LFMC estimation RMSE difference is very small (≈5%, $p = 0.0002$). An outlier (fuel type: oak, site: City of Austin-Onion) is seen in SACC (shown by the red dot), where the correlation coefficient derived using SCAN data is significantly smaller. It is worth noting that the other fuel type (juniper) at this site also demonstrates large difference in the correlation analysis (ECV_SM: 0.54, SCAN: 0.27). The plot also reveals that the utility of the ordinary regression is significantly undermined by the presence of the outlier, and that the robust regression effectively eliminates the influence, which justifies the use of robust regression in this study. It is also worth noting that the correlation coefficients derived using SCAN data are generally higher than those derived using ECV_SM data, which may relate to a better representation of soil moisture dynamics at the LFMC sampling site.

3.4. LFMC ~ ECV_SM correlation under different aridity conditions

Fig. 7 shows the observed and estimated LFMC at some sites in different GACCs. The figure demonstrates that using soil moisture as a predictor, the estimated LFMC follows the overall temporal dynamics of the observations. The estimates agree with observations when the LFMC is low to medium, but the estimation performance deteriorates when

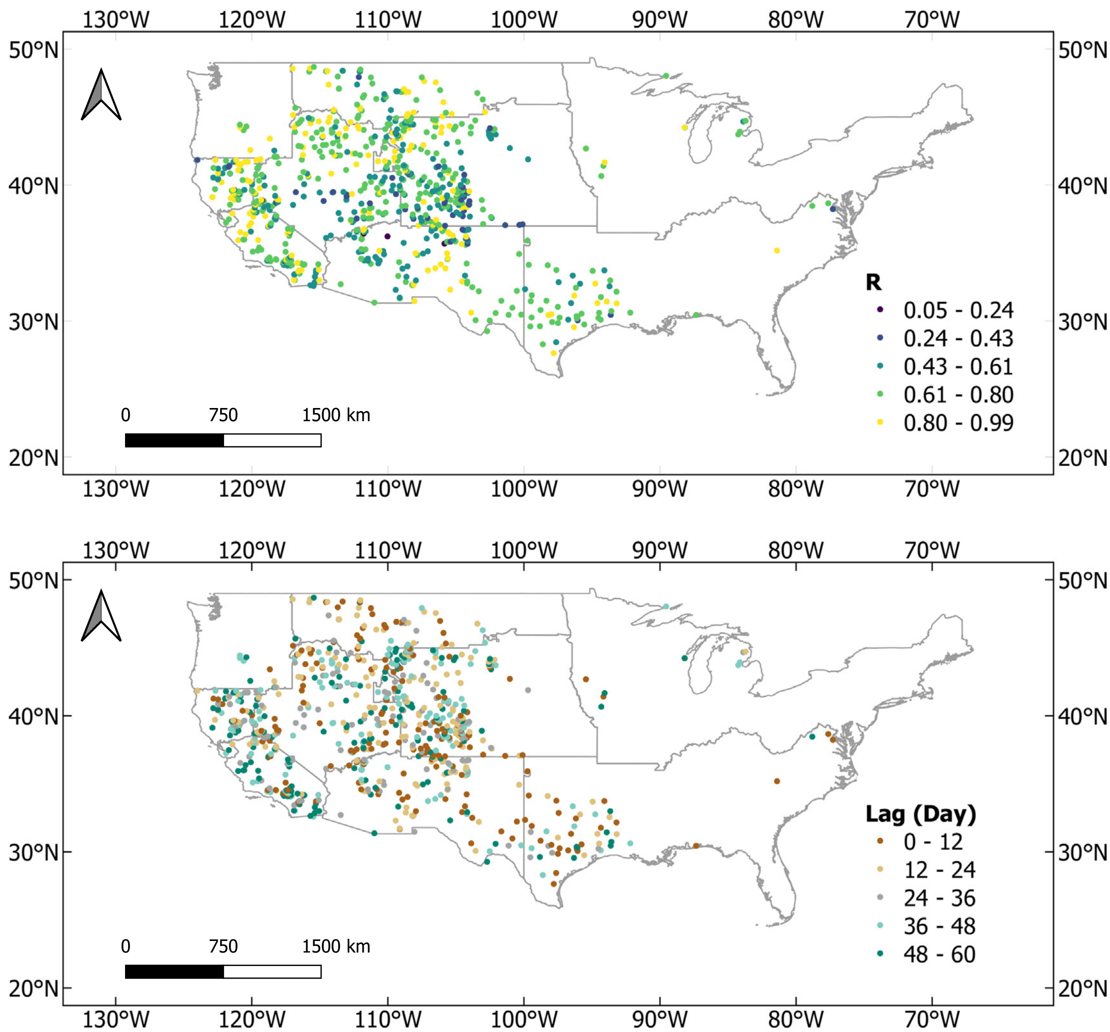

Fig. 5. Spatial patterns of LFMC ~ ECV_SM correlation coefficients and optimal time lags over the coterminous United States.

the LFMC is high. Here the method was re-implemented for the lowest (i.e., driest) 50%, 40%, 30%, 20% and 10% of LFMC samplings separately, which were adopted as proxies for dry spells of different aridity. It should be noted that the LFMC sampling sites analyzed in each category were not the same as a result of the quality control procedure. For example, sites with over 25 LFMC and soil moisture records were included in the lowest 40% analysis, while only sites with over 100 records were used in the lowest 10% analysis to guarantee that at least 10 LFMC ~ soil moisture data pairs were available for the evaluation.

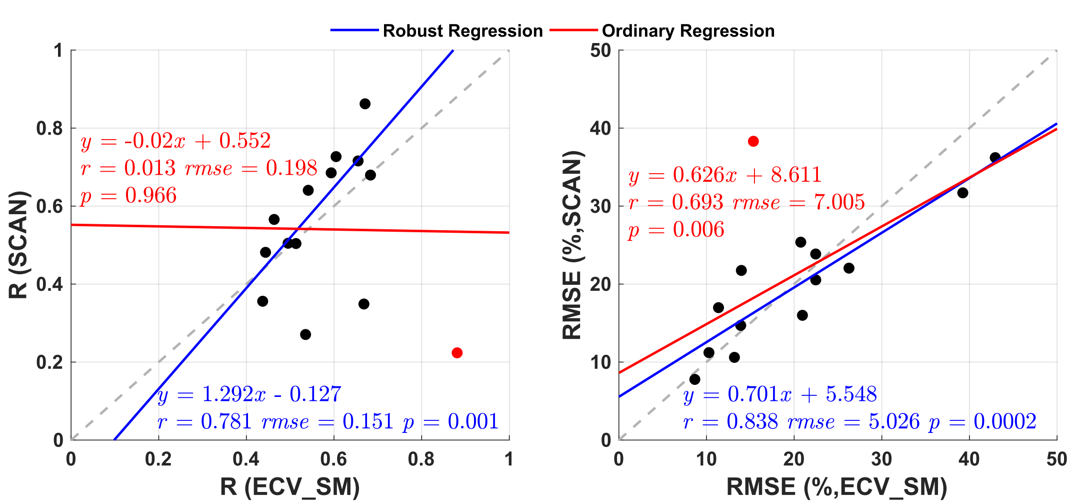

Fig. 6. Comparison of the correlation coefficients and RMSEs derived using ECV_SM and SCAN data for 14 fuel types at 7 sites. The red dot indicates the outlier. (For interpretation of the references to colour in this figure legend, the reader is referred to the web version of this article.)

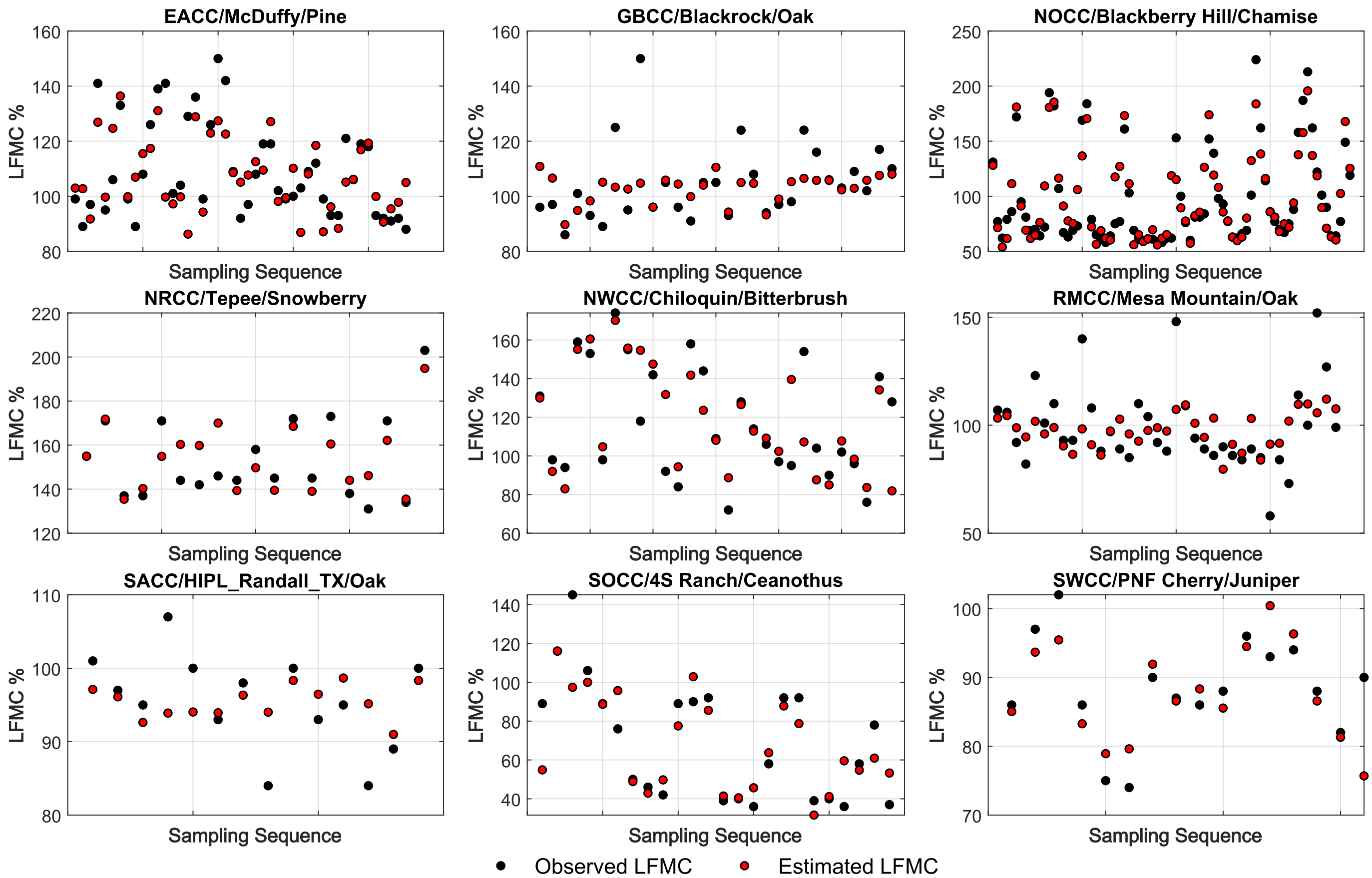

Fig. 7. Observed and estimated LFMC at some sites in different GACCs. The GACC acronyms are listed in Table 1. The sub-graphs are named after "GACC/site name/fuel type".

The median values of the statistical metrics in each GACC are included in Table 3, and the results are also included in Fig. S1 in the Supplementary materials. In most GACCs, an increasing trend in the correlation coefficient is observed with decreasing LFMC values. Meanwhile, the LFMC estimation RMSE decreases with lower LFMC in all GACCs, and is mostly under 5% for the lowest 20% of LFMC samplings. In particular, a strong decreasing trend with higher aridity is also observed in nRMSE in all GACCs. For the lowest 20% of LFMC samplings, the estimation RMSE is mostly below 5%.

3.5. Inter-annual variability of LFMC ~ ECV_SM correlation

One issue that would affect the applicability of the LFMC ~ soil moisture relationship trained using historical data in LFMC prediction is the inter-annual stability of the relationship. The predictive utility of the trained model will be undermined if large variability exists in the LFMC ~ soil moisture correlation in different years. Here the temporal variation of the annual correlation coefficients from 1979 to 2018 was derived for each GACC and the coterminous United States (shown in Fig. S2 in the Supplementary materials). Prior to year 2003, the evaluation is mainly constrained by the limited availability of satellite soil moisture data and LFMC samplings, and the correlation coefficients in general demonstrate large inter-annual variations as a result of the small data set. With more satellite data becoming available, the correlation generally stabilizes, particularly in recent years. Over the coterminous United States, the overall median value is between 0.7 and 0.8, and has been mostly stable in the past decade. This suggests that the LFMC and soil moisture correlation is mostly independent of the year, and that the model trained with historical data can be used for LFMC prediction in the future.

Table 3
Median values for R, RMSE and nRMSE in each GACC. The GACC acronyms are listed in Table 1. The metrics are for the lowest 50%, 40%, 30%, 20% and 10% of LFMC samplings from left to right. The best performance in each category is highlighted in bold.

GACC	Median R	Median RMSE %	Median nRMSE
EACC	0.68/**0.79**/**0.79**/0.73/0.75	8.54/5.09/3.55/3.36/**1.67**	0.08/0.05/0.04/0.03/**0.02**
GBCC	0.61/0.63/0.66/0.70/**0.73**	8.09/6.81/6.14/5.09/**3.92**	0.09/0.07/0.08/0.06/**0.05**
NOCC	0.63/0.62/0.66/**0.73**/0.60	7.59/5.46/4.47/3.67/**3.62**	0.09/0.07/0.06/**0.05**/**0.05**
NRCC	0.74/0.77/0.73/**0.80**/0.79	7.56/6.38/6.12/2.74/**0.97**	0.07/0.06/0.06/0.03/**0.01**
NWCC	0.53/0.48/0.51/0.66/**0.71**	10.37/9.12/7.98/5.26/**3.32**	0.14/0.13/0.11/0.08/**0.05**
RMCC	0.65/0.68/0.71/0.74/**0.79**	6.78/5.84/4.43/3.91/**3.18**	0.07/0.07/0.05/0.05/**0.04**
SACC	0.65/0.69/0.72/0.76/**0.79**	7.17/5.86/4.58/4.05/**3.94**	0.07/0.06/**0.05**/**0.05**/0.05
SOCC	0.59/0.63/0.70/**0.75**/**0.75**	6.02/4.91/3.61/2.95/**1.67**	0.10/0.08/0.06/0.06/**0.03**
SWCC	0.64/0.72/0.74/**0.81**/**0.81**	5.84/4.84/4.28/3.90/**2.67**	0.07/0.06/0.05/0.05/**0.03**

3.6. Utility of surface vs. root-zone soil moisture

To evaluate if root-zone soil moisture outperforms surface soil moisture in LFMC estimation, their respective explanatory utility was compared using SMAP Level-4 product between March 31, 2015 and June 30, 2018, and the ECV_SM results are also plotted as a reference (shown in Fig. S3 in the Supplementary materials). Overall, the correlation coefficients derived using SMAP Level-4 surface or root-zone soil moisture are comparable, while the correlation tends to have a wider spread when root-zone soil moisture is used. Compared with ECV_SM, the correlation coefficients using SMAP Level-4 product are generally higher, which may relate to the better depiction of soil moisture dynamics thanks to the higher resolution of SMAP Level-4 product (9 km) compared to the ECV_SM product (≈25 km). The estimation RMSE is also similar, and the RMSE range in each GACC agrees well with those derived using ECV_SM data. As plant roots can make use of root-zone soil moisture directly, the estimated time lags for root-zone soil moisture are smaller than those for SMAP Level-4 surface soil moisture and ECV_SM. The SMAP Level-4 surface soil moisture time lags generally agree with those for ECV_SM (e.g, largest in SOCC and NOCC, and smallest in SACC), but notable differences exist in some regions (e.g., in EACC). This may be caused by the ECV_SM data gap or the difference in data resolution. Overall, the SMAP Level-4 surface slightly outperforms ECV_SM and performs similarly with root-zone soil moisture data in LFMC estimation.

4. Discussion

4.1. Performance of the time-lagged analysis

Previous studies have found that the response of vegetation to climate has a certain time lag (Davis, 1989; Kuzyakov and Gavrichkova, 2010; Vicente-Serrano et al., 2013; Chen et al., 2014). The time-lagged time series analysis has so far been widely used to evaluate the relationship between climatic drivers and vegetation development. At regional level, Chen et al. (2014) found that vegetation typically responses to soil moisture lagged by approximately one month in mainland Australia, and a study in southern China found that the time lag of vegetation response to soil moisture varies from under 16 days to as long as 96 days (Niu et al., 2018). At global scale, Wu et al. (2015) found that vegetation time-lag to precipitation varies with region within 3 months.

This study is based on the statistical analysis between LFMC observations and time-lagged soil moisture data within a 60-day threshold, which is determined based on a sensitivity analysis of the maximum correlation achievable. This suggests that at most sites the LFMC correlates best with the soil moisture condition within 60 days before the LFMC sampling date, and that increasing the threshold to 100 days has negligible benefits as the highest correlation has already been achieved within a 60-day time lag. By definition a larger lag threshold may lead to higher correlation coefficients, but the improvement may be caused by over-fitting and may lack grounds in plant physiology. The threshold is sufficiently large for most areas in the coterminous United States (Wu et al., 2015), and the correlation is significant ($p < 0.01$) at most sites. The estimated optimal lags for individual fuel types may be difficult to interpret, since plant water content variations are related to both local climatic conditions and the ecological characteristics of the plant species (Castro et al., 2003; Pellizzaro et al., 2007). Over most GACCs, the median of optimal lags is between 20 and 40 days, which is consistent with a study that suggests a one-month lag for grass in Kansas (Rundquist and Harrington Jr, 2000). The lag is the longest in southern California and many sites have lags longer than 50 days, which agrees with the two-month lag reported in Jia et al. (2019). It should be noted that more physically-based understanding and interpretation of the time lag is still lacking in literature, and more work on the role of soil moisture on plant physiology should be done to improve the characterization of vegetation response to soil moisture variation.

4.2. LFMC predictability under different conditions

Fig. 7 and Table 3 demonstrate that soil moisture has higher explanatory utility on LFMC under higher aridity conditions. This finding is very promising and may have important implications on LFMC estimation for wildfire risk assessment. Previous studies have suggested that fire danger dramatically increases when LFMC drops below a certain threshold (Dennison et al., 2008), and multiple fire classification standards have been proposed for different regions and fuel types (Green, 1981; Weise et al., 1998; Schoenberg et al., 2003; Dennison et al., 2008). As the fire danger is usually low for high LFMC values, the relatively larger LFMC estimation error is expected to have small impacts on fire danger assessment. In contrast, as low LFMC values can be predicted by soil moisture with higher accuracy, the areas with high fire dangers can be better monitored thanks to the larger impact of soil moisture on LFMC variation under drier conditions.

The comparison using surface and root-zone soil moisture suggests that their respective predictive utility on LFMC is comparable. The finding is consistent with Jia et al. (2019) from a similar experiment in southern California. Since SMAP Level-4 product is derived by assimilating SMAP brightness temperature measurements into the physically-based Catchment land surface model (Koster et al., 2000), the deeper-layer soil moisture interacts actively with the surface layer. As a result, the surface and root-zone soil moisture are temporally correlated, thus the added value of root-zone soil moisture is limited in the regression-based analysis. Previous studies have also demonstrated a good correlation between surface and profile moisture (Albergel et al., 2008). It is worth noting that the finding is different from Fan et al. (2018), who found that LFMC has a higher correlation with root-zone soil moisture derived from ECV_SM using an exponential filter in the Mediterranean region.

4.3. Influential factors on the evaluation

A spatial resolution gap exists between remote sensing soil moisture data and point-level LFMC samplings as well as between ECV_SM and SMAP Level-4 product, which may have some influence on the evaluation. The influence may be noticeable over complex terrain, where the soil moisture measurements are more susceptible to topography effect and land-use heterogeneity (Pasolli et al., 2014), and the spatial representativeness is also complicated by the large spatial heterogeneity of soil moisture (Williams et al., 2009; Bertoldi et al., 2014). In addition, when soil moisture is retrieved from C-band synthetic aperture radar (e.g., ASCAT), the backscatter is also influenced by the incidence angle (Naeimi et al., 2009), surface roughness (Kornelsen and Coulibaly, 2013) and dense vegetation (El Hajj et al., 2019). This is in some sense unavoidable since LFMC cannot be upscaled to the pixel scale and soil moisture data are currently unavailable at very fine resolution. The influence is expected to be manageable, as the temporal dynamics of soil moisture has a larger impact than the exact value in determining the model performance in a regression-based analysis. Soil moisture temporal variation is mainly driven by precipitation patterns, which are generally similar within the ECV_SM pixel scale (≈25 km) (Crow et al., 2012). Evaluation studies overall suggest a high temporal correlation between remote sensing soil moisture data and in situ data (Dorigo et al., 2015; Pan et al., 2016), and a recent study demonstrates that sparse network is able to provide unbiased evaluation of soil moisture climatology when averaged regionally (Dong et al., 2020). Therefore remote sensing soil moisture is expected to well represent the soil moisture temporal dynamics within the pixel in most cases.

The LFMC samplings from the NFMD were mainly collected during summer and autumn, and the sites are predominantly located in the western United States. This is in line with the major fire season and the wildfire-active regions (Dennison et al., 2014). Some studies have suggested that soil moisture has a reduced influence on LFMC during the dormant season as the plants are dead or dormant (Krueger et al., 2015). Under this condition, the weather condition is expected to play a larger role on wildfire occurrence.

4.4. Implications on LFMC estimation using soil moisture

Nolan et al. (2016) suggested that the transformation of fuel moisture can occur within a month which can dramatically change the wildfire risk, and highlighted the need for a high temporal resolution monitoring system. In this study, soil moisture measurements from microwave remote sensing prove to be well correlated to LFMC data over the coterminous United States, which provides potential for the construction of a LFMC estimation system at daily scale on this basis. However, the satellite revisit interval is typically 2–3 days for passive microwave sensing (Kerr et al., 2001; Entekhabi et al., 2010), and can be even longer for active radar sensing as a result of the higher spatial resolution (Torres et al., 2012), leaving observation gaps in the daily composite. The similar performance of SMAP Level-4 product in LFMC estimation suggests that soil moisture data based on land surface modelling and data assimilation, such as the SMAP Level-4 product and data from the North America Land Data Assimilation System (Mitchell et al., 2004; Xia et al., 2012), may be used as a substitute for remote sensing soil moisture in LFMC estimation. Recently, Yebra et al. (2019) generated a LFMC database based on data samplings from 1383 sites in 11 countries, which could be used to train and validate soil moisture-based prediction models over large areas. These would potentially enable spatio-temporally consistent LFMC estimation at continental or even global scale. In addition, it is worth noting that the soil moisture correlation with LFMC derived using SCAN or SMAP Level-4 data tends to be higher than that using ECV_SM data, which may relate to a better characterization of soil moisture variability at finer resolution. This implies that the true LFMC and soil moisture coupling may be higher at point scale, and that finer resolution soil moisture products may have higher explanatory capacity on LFMC. A comparison of Figs. 2 and 3 indicates that in some regions (e.g., SACC and SWCC), one site can feature multiple fuel types with different response intensities to soil moisture variation, otherwise the distribution of correlation for all fuel types should be comparable with the correlation for the high-response fuel types, while in some other regions (e.g., NWCC and NOCC) the LFMC and soil moisture correlation is mostly uniform among different fuel types.

4.5. Implications on wildfire risk assessment

The findings from this study are important for wildfire risk assessment. Wildfire risk can be quantified from three aspects - the ignition potential, the availability of fuels and the rate of fire spread once initiated (Preisler et al., 2004; Miller and Ager, 2013), which are all affected by LFMC. Hence an accurate estimation for LFMC would greatly facilitate wildfire risk assessment and loss reduction. Results from this study demonstrate that LFMC is robustly correlated to previous soil moisture condition, which suggests that the current soil moisture condition may be used to predict LFMC from a couple of days later to as long as 2 months later depending on the site and fuel type. The LFMC forecast period can be further extended if the prediction is combined with a land surface forecast system. In addition, the results demonstrate that soil moisture has higher explanatory utility for lower LFMC, which is usually related to higher wildfire risk. This suggests that soil moisture condition may be particularly informative in predicting imminent large wildfire risks. With a wildfire risk assessment based on LFMC estimates, wildfire precautions may be deployed and resources distributed prior to fire occurrence.

Here a linear regression model is adopted for LFMC estimation, and only soil moisture is used as the predictive variable. This serves as the basis upon which more sophisticated models can be built and more variables with complementary information on LFMC can be included. Other studies have suggested that non-linear models perform better than linear models (Nolan et al., 2016), and that variables such as cumulative growing degree days (Jia et al., 2019), visible atmospheric resistant index (Fan et al., 2018) and surface reflectance (Yebra et al., 2018) can be used to improve LFMC prediction. A recent study found that the combination of soil moisture and vapor pressure deficit (VPD) effectively improves wildfire prediction (Rigden et al., 2020). Some landscape characteristics such as elevation and slope also have large impacts on model performance (Rao et al., 2020). Other variables related to vegetation physiology may also refine model simulation, such as evapotranspiration data based on disaggregated land surface simulation (Anderson et al., 2011), data assimilation (Lu et al., 2017, 2020), and foliage relative water content (Nolan et al., 2020). In particular, the recent ECOSTRESS mission has the capacity to provide evapotranspiration data at 70 m resolution every 1–5 days, which may have strong potential for LFMC prediction (Fisher et al., 2020). Recently, Rao et al. (2020) proposed a physics-assisted recurrent neural network model for LFMC estimation which used microwave backscatter and optical reflectance data as well as ancillary data such as soil texture and slope. The model was able to derive accurate LFMC estimates at 250 m resolution every 15 days. This suggests that new models that combine strengths of physical and empirical approaches may further improve LFMC prediction over purely empirical or physical methods.

5. Conclusion

In this study, a comprehensive evaluation of the utility of microwave soil moisture data on LFMC estimation was conducted over the coterminous United States using a time-lagged robust linear regression method. The analysis was first performed using the ECV_SM product and LFMC measurements from over 1000 sites between 1979 and 2018 for different fuel types. The evaluation was verified using in situ soil moisture data from SCAN, and the utility of surface and root-zone soil moisture was compared using the SMAP Level-4 product which is derived from microwave data assimilation.

An analysis with different time lag thresholds suggested that at most sites, the LFMC correlates best with soil moisture data within 60 days prior to the sampling date. In most regions, the LFMC is significantly correlated to soil moisture (p<0.01), and the average estimation RMSE is around 20%. The correlation appears to be lower in areas with complex terrain, and the optimal time lag depends on the region and vegetation type. The major fuel types with a high response to soil moisture include pine, redcedar, sagebrush, oak, manzanita, chamise, mesquite and juniper, depending on the region. The analysis using in situ SCAN data yields similar results. Further analyses showed that soil moisture has higher explanatory utility for lower LFMC, and that the correlation is mostly stable among different years. Despite a closer relationship with vegetation growth, root-zone soil moisture has comparable performance with surface soil moisture in LFMC estimation. This study demonstrated that microwave soil moisture data contain sufficient information for LFMC estimation over the coterminous United States, which provides a good basis upon which more sophisticated models with more predictive variables can be developed.

CRediT authorship contribution statement

Yang Lu: Software, Visualization, Writing – review & editing. **Chunzhu Wei:** Conceptualization, Methodology, Writing – review & editing.

Declaration of competing interest

The authors declare that they have no known competing financial interests or personal relationships that could have appeared to influence the work reported in this paper.

Acknowledgements

This research was supported by the National Natural Science Foundation of China (No. 42001178 and 41930646) and the Fundamental Research Funds for the Central Universities (No. 37000-31610452).

Appendix A. Supplementary data

Supplementary data to this article can be found online at https://doi.org/10.1016/j.scitotenv.2021.145410.

References

Albergel, C., Rüdiger, C., Pellarin, T., Calvet, J.C., Fritz, N., Froissard, F., Suquia, D., Petitpa, A., Piguet, B., Martin, E., 2008. From near-surface to root-zone soil moisture using an exponential filter: an assessment of the method based on in-situ observations and model simulations. Hydrol. Earth Syst. Sci. 12, 1323–1337.

Anderson, M., Kustas, W., Norman, J., Hain, C., Mecikalski, J., Schultz, L., González-Dugo, M., Cammalleri, C., d'Urso, G., Pimstein, A., et al., 2011. Mapping daily evapotranspiration at field to continental scales using geostationary and polar orbiting satellite imagery. Hydrol. Earth Syst. Sci. 15, 223–239.

Bartalis, Z., Wagner, W., Naeimi, V., Hasenauer, S., Scipal, K., Bonekamp, H., Figa, J., Anderson, C., 2007. Initial soil moisture retrievals from the METOP-A Advanced Scatterometer (ASCAT). Geophysical Research Letters 34.

Bertoldi, G., Della Chiesa, S., Notarnicola, C., Pasolli, L., Niedrist, G., Tappeiner, U., 2014. Estimation of soil moisture patterns in mountain grasslands by means of SAR RADARSAT2 images and hydrological modeling. J. Hydrol. 516, 245–257.

Brocca, L., Ciabatta, L., Moramarco, T., Ponziani, F., Berni, N., Wagner, W., 2016. Use of satellite soil moisture products for the operational mitigation of landslides risk in central Italy, in: Satellite Soil Moisture Retrieval. Elsevier, pp. 231–247.

Castro, F., Tudela, A., Sebastià, M.T., 2003. Modeling moisture content in shrubs to predict fire risk in Catalonia (Spain). Agric. For. Meteorol. 116, 49–59.

Ceccato, P., Gobron, N., Flasse, S., Pinty, B., Tarantola, S., 2002. Designing a spectral index to estimate vegetation water content from remote sensing data: part 1: theoretical approach. Remote Sens. Environ. 82, 188–197.

Chen, T., De Jeu, R., Liu, Y., Van der Werf, G., Dolman, A., 2014. Using satellite based soil moisture to quantify the water driven variability in NDVI: a case study over mainland Australia. Remote Sens. Environ. 140, 330–338.

Chuvieco, E., Riaño, D., Aguado, I., Cocero, D., 2002. Estimation of fuel moisture content from multitemporal analysis of Landsat Thematic Mapper reflectance data: applications in fire danger assessment. Int. J. Remote Sens. 23, 2145–2162.

Colliander, A., Jackson, T.J., Bindlish, R., Chan, S., Das, N., Kim, S., Cosh, M., Dunbar, R., Dang, L., Pashaian, L., et al., 2017. Validation of SMAP surface soil moisture products with core validation sites. Remote Sens. Environ. 191, 215–231.

Countryman, C.M., Dean, W.A., 1979. Measuring Moisture Content in Living Chaparral: A Field User's Manual. vol. 36. US Department of Agriculture, Forest Service, Pacific Southwest Forest and Range Experiment Station.

Crow, W.T., Berg, A.A., Cosh, M.H., Loew, A., Mohanty, B.P., Panciera, R., de Rosnay, P., Ryu, D., Walker, J.P., 2012. Upscaling sparse ground-based soil moisture observations for the validation of coarse-resolution satellite soil moisture products. Reviews of Geophysics 50.

Danson, F.M., Bowyer, P., 2004. Estimating live fuel moisture content from remotely sensed reflectance. Remote Sens. Environ. 92, 309–321.

Davis, M.B., 1989. Lags in vegetation response to greenhouse warming. Clim. Chang. 15, 75–82.

de Jeu, R., Dorigo, W., 2016. On the importance of satellite observed soil moisture. Int. J. Appl. Earth Obs. Geoinf. 45, 107–109.

Deeming, J.E., 1972. National Fire-danger Rating System. vol. 84. Rocky Mountain Forest and Range Experiment Station, Forest Service, US Department of Agriculture.

Dennison, P.E., Roberts, D.A., Thorgusen, S.R., Regelbrugge, J.C., Weise, D., Lee, C., 2003. Modeling seasonal changes in live fuel moisture and equivalent water thickness using a cumulative water balance index. Remote Sens. Environ. 88, 442–452.

Dennison, P., Roberts, D., Peterson, S., Rechel, J., 2005. Use of normalized difference water index for monitoring live fuel moisture. Int. J. Remote Sens. 26, 1035–1042.

Dennison, P.E., Moritz, M.A., Taylor, R.S., 2008. Evaluating predictive models of critical live fuel moisture in the Santa Monica Mountains, California. Int. J. Wildland Fire 17, 18–27.

Dennison, P.E., Brewer, S.C., Arnold, J.D., Moritz, M.A., 2014. Large wildfire trends in the western United States, 1984–2011. Geophys. Res. Lett. 41, 2928–2933.

Dimitrakopoulos, A., Bemmerzouk, A., 2003. Predicting live herbaceous moisture content from a seasonal drought index. Int. J. Biometeorol. 47, 73–79.

Dong, J., Crow, W.T., Tobin, K.J., Cosh, M.H., Bosch, D.D., Starks, P.J., Seyfried, M., Collins, C.H., 2020. Comparison of microwave remote sensing and land surface modeling for surface soil moisture climatology estimation. Remote Sens. Environ. 242, 111756.

Donovan, V.M., Wonkka, C.L., Twidwell, D., 2017. Surging wildfire activity in a grassland biome. Geophys. Res. Lett. 44, 5986–5993.

Dorigo, W., Gruber, A., De Jeu, R., Wagner, W., Stacke, T., Loew, A., Albergel, C., Brocca, L., Chung, D., Parinussa, R., et al., 2015. Evaluation of the ESA CCI soil moisture product using ground-based observations. Remote Sens. Environ. 162, 380–395.

El Hajj, M., Baghdadi, N., Zribi, M., 2019. Comparative analysis of the accuracy of surface soil moisture estimation from the C-and L-bands. Int. J. Appl. Earth Obs. Geoinf. 82, 101888.

Entekhabi, D., Njoku, E.G., O'Neill, P.E., Kellogg, K.H., Crow, W.T., Edelstein, W.N., Entin, J.K., Goodman, S.D., Jackson, T.J., Johnson, J., et al., 2010. The soil moisture active passive (SMAP) mission. Proc. IEEE 98, 704–716.

Fan, L., Xiao, Q., Wen, J., Liu, Q., Tang, Y., You, D., Wang, H., Gong, Z., Li, X., 2015. Evaluation of the airborne CASI/TASI Ts-VI space method for estimating near-surface soil moisture. Remote Sens. 7, 3114–3137.

Fan, L., Wigneron, J.P., Xiao, Q., Al-Yaari, A., Wen, J., Martin-StPaul, N., Dupuy, J.L., Pimont, F., Al Bitar, A., Fernandez-Moran, R., et al., 2018. Evaluation of microwave remote sensing for monitoring live fuel moisture content in the Mediterranean region. Remote Sens. Environ. 205, 210–223.

Fares, S., Bajocco, S., Salvati, L., Camarretta, N., Dupuy, J.L., Xanthopoulos, G., Guijarro, M., Madrigal, J., Hernando, C., Corona, P., 2017. Characterizing potential wildland fire fuel in live vegetation in the Mediterranean region. Ann. For. Sci. 74, 1.

Fisher, J.B., Lee, B., Purdy, A.J., Halverson, G.H., Dohlen, M.B., Cawse-Nicholson, K., Wang, A., Anderson, R.G., Aragon, B., Arain, M.A., et al., 2020. ECOSTRESS: NASA's next generation mission to measure evapotranspiration from the International Space Station. Water Resources Research 56, e2019WR026058.

Gao, B.C., 1996. NDWI—a normalized difference water index for remote sensing of vegetation liquid water from space. Remote Sens. Environ. 58, 257–266.

García, M., Chuvieco, E., Nieto, H., Aguado, I., 2008. Combining AVHRR and meteorological data for estimating live fuel moisture content. Remote Sens. Environ. 112, 3618–3627.

Giglio, L., Boschetti, L., Roy, D.P., Humber, M.L., Justice, C.O., 2018. The collection 6 MODIS burned area mapping algorithm and product. Remote Sens. Environ. 217, 72–85.

González-Zamora, Á., Sánchez, N., Martínez-Fernández, J., Wagner, W., 2016. Root-zone plant available water estimation using the SMOS-derived soil water index. Adv. Water Resour. 96, 339–353.

Green, L.R., 1981. Burning by Prescription in Chaparral. vol. 51. US Department of Agriculture, Forest Service, Pacific Southwest Forest and Range Experiment Station.

Gruber, A., Scanlon, T., van der Schalie, R., Wagner, W., Dorigo, W., 2019. Evolution of the ESA CCI soil moisture climate data records and their underlying merging methodology. Earth System Science Data 1–37.

Jia, S., Kim, S.H., Nghiem, S.V., Kafatos, M., 2019. Estimating live fuel moisture using SMAP L-band radiometer soil moisture for Southern California, USA. Remote Sens. 11, 1575.

Jolly, W.M., 2007. Sensitivity of a surface fire spread model and associated fire behaviour fuel models to changes in live fuel moisture. Int. J. Wildland Fire 16, 503–509.

Jolly, W.M., Johnson, D.M., 2018. Pyro-ecophysiology: shifting the paradigm of live wildland fuel research. Fire 1, 8.

Jolly, W.M., Hadlow, A.M., Huguet, K., 2014. De-coupling seasonal changes in water content and dry matter to predict live conifer foliar moisture content. Int. J. Wildland Fire 23, 480–489.

Jolly, W.M., Cochrane, M.A., Freeborn, P.H., Holden, Z.A., Brown, T.J., Williamson, G.J., Bowman, D.M., 2015. Climate-induced variations in global wildfire danger from 1979 to 2013. Nat. Commun. 6, 1–11.

Karavani, A., Boer, M.M., Baudena, M., Colinas, C., Daz-Sierra, R., Pemán, J., de Luis, M., Enrquez-de Salamanca, Á., Resco de Dios, V., 2018. Fire-induced deforestation in drought-prone Mediterranean forests: drivers and unknowns from leaves to communities. Ecol. Monogr. 88, 141–169.

Keetch, J.J., Byram, G.M., 1968. A Drought Index for Forest Fire Control. vol. 38. US Department of Agriculture, Forest Service.

Kelley, D.I., Bistinas, I., Whitley, R., Burton, C., Marthews, T.R., Dong, N., 2019. How contemporary bioclimatic and human controls change global fire regimes. Nat. Clim. Chang. 9, 690–696.

Kerr, Y.H., Waldteufel, P., Wigneron, J.P., Martinuzzi, J., Font, J., Berger, M., 2001. Soil moisture retrieval from space: the soil moisture and ocean salinity (SMOS) mission. IEEE Trans. Geosci. Remote Sens. 39, 1729–1735.

Kornelsen, K.C., Coulibaly, P., 2013. Advances in soil moisture retrieval from synthetic aperture radar and hydrological applications. J. Hydrol. 476, 460–489.

Koster, R.D., Suarez, M.J., Ducharne, A., Stieglitz, M., Kumar, P., 2000. A catchment-based approach to modeling land surface processes in a general circulation model: 1. Model structure. Journal of Geophysical Research: Atmospheres 105, 24809–24822.

Krueger, E.S., Ochsner, T.E., Engle, D.M., Carlson, J., Twidwell, D., Fuhlendorf, S.D., 2015. Soil moisture affects growing-season wildfire size in the Southern Great Plains. Soil Sci. Soc. Am. J. 79, 1567–1576.

Kuzyakov, Y., Gavrichkova, O., 2010. Time lag between photosynthesis and carbon dioxide efflux from soil: a review of mechanisms and controls. Glob. Chang. Biol. 16, 3386–3406.

Liu, Y., Stanturf, J., Goodrick, S., 2010. Trends in global wildfire potential in a changing climate. For. Ecol. Manag. 259, 685–697.

Lu, Y., Steele-Dunne, S.C., Farhadi, L., van de Giesen, N., 2017. Mapping surface heat fluxes by assimilating SMAP soil moisture and GOES land surface temperature data. Water Resour. Res. 53, 10858–10877.

Lu, Y., Steele-Dunne, S.C., De Lannoy, G.J., 2020. Improving soil moisture and surface turbulent heat flux estimates by assimilation of SMAP brightness temperatures or soil moisture retrievals and GOES land surface temperature retrievals. J. Hydrometeorol. 21, 183–203.

Miller, C., Ager, A.A., 2013. A review of recent advances in risk analysis for wildfire management. Int. J. Wildland Fire 22, 1–14.

Mitchell, K.E., Lohmann, D., Houser, P.R., Wood, E.F., Schaake, J.C., Robock, A., Cosgrove, B.A., Sheffield, J., Duan, Q., Luo, L., et al., 2004. The multi-institution North American Land Data Assimilation System (NLDAS): utilizing multiple GCIP products and partners in a continental distributed hydrological modeling system. Journal of Geophysical Research: Atmospheres 109.

Myoung, B., Kim, S.H., Nghiem, S.V., Jia, S., Whitney, K., Kafatos, M.C., 2018. Estimating live fuel moisture from MODIS satellite data for wildfire danger assessment in Southern California USA. Remote Sens. 10, 87.

Naeimi, V., Bartalis, Z., Wagner, W., 2009. ASCAT soil moisture: an assessment of the data quality and consistency with the ERS scatterometer heritage. J. Hydrometeorol. 10, 555–563.

Niu, J., Chen, J., Sun, L., Sivakumar, B., 2018. Time-lag effects of vegetation responses to soil moisture evolution: a case study in the Xijiang basin in South China. Stoch. Env. Res. Risk A. 32, 2423–2432.

Njoku, E.G., Jackson, T.J., Lakshmi, V., Chan, T.K., Nghiem, S.V., 2003. Soil moisture retrieval from AMSR-E. IEEE Trans. Geosci. Remote Sens. 41, 215–229.

Nolan, R.H., Boer, M.M., Resco de Dios, V., Caccamo, G., Bradstock, R.A., 2016. Large-scale, dynamic transformations in fuel moisture drive wildfire activity across southeastern Australia. Geophys. Res. Lett. 43, 4229–4238.

Nolan, R.H., Blackman, C.J., de Dios, V.R., Choat, B., Medlyn, B.E., Li, X., Bradstock, R.A., Boer, M.M., 2020. Linking forest flammability and plant vulnerability to drought. Forests 11, 779.

Pan, M., Cai, X., Chaney, N.W., Entekhabi, D., Wood, E.F., 2016. An initial assessment of SMAP soil moisture retrievals using high-resolution model simulations and in situ observations. Geophys. Res. Lett. 43, 9662–9668.

Pasolli, L., Notarnicola, C., Bertoldi, G., Della Chiesa, S., Niedrist, G., Bruzzone, L., Tappeiner, U., Zebisch, M., 2014. Soil moisture monitoring in mountain areas by using high-resolution SAR images: results from a feasibility study. Eur. J. Soil Sci. 65, 852–864.

Pellizzaro, G., Cesaraccio, C., Duce, P., Ventura, A., Zara, P., 2007. Relationships between seasonal patterns of live fuel moisture and meteorological drought indices for Mediterranean shrubland species. Int. J. Wildland Fire 16, 232–241.

Peterson, S.H., Roberts, D.A., Dennison, P.E., 2008. Mapping live fuel moisture with MODIS data: a multiple regression approach. Remote Sens. Environ. 112, 4272–4284.

Preisler, H.K., Brillinger, D.R., Burgan, R.E., Benoit, J., 2004. Probability based models for estimation of wildfire risk. Int. J. Wildland Fire 13, 133–142.

Qi, Y., Dennison, P.E., Spencer, J., Riaño, D., 2012. Monitoring live fuel moisture using soil moisture and remote sensing proxies. Fire Ecology 8, 71.

Rao, K., Williams, A.P., Flefil, J.F., Konings, A.G., 2020. SAR-enhanced mapping of live fuel moisture content. Remote Sens. Environ. 245, 111797.

Reichle, R.H., De Lannoy, G.J., Liu, Q., Ardizzone, J.V., Colliander, A., Conaty, A., Crow, W., Jackson, T.J., Jones, L.A., Kimball, J.S., et al., 2017a. Assessment of the SMAP Level-4 surface and root-zone soil moisture product using in situ measurements. J. Hydrometeorol. 18, 2621–2645.

Reichle, R.H., De Lannoy, G.J., Liu, Q., Koster, R.D., Kimball, J.S., Crow, W.T., Ardizzone, J.V., Chakraborty, P., Collins, D.W., Conaty, A.L., et al., 2017b. Global assessment of the SMAP Level-4 surface and root-zone soil moisture product using assimilation diagnostics. J. Hydrometeorol. 18, 3217–3237.

Rigden, A.J., Powell, R.S., Trevino, A., McColl, K.A., Huybers, P., 2020. Microwave Retrievals of Soil Moisture Improve Grassland Wildfire Predictions 47, e2020GL091410.

Rossa, C.G., 2017. The effect of fuel moisture content on the spread rate of forest fires in the absence of wind or slope. Int. J. Wildland Fire 26, 24–31.

Rossa, C.G., Veloso, R., Fernandes, P.M., 2016. A laboratory-based quantification of the effect of live fuel moisture content on fire spread rate. Int. J. Wildland Fire 25, 569–573.

Ruffault, J., Martin-StPaul, N., Pimont, F., Dupuy, J.L., 2018. How well do meteorological drought indices predict live fuel moisture content (LFMC)? An assessment for wildfire research and operations in Mediterranean ecosystems. Agric. For. Meteorol. 262, 391–401.

Rundquist, B.C., Harrington Jr., J.A., 2000. The effects of climatic factors on vegetation dynamics of tallgrass and shortgrass cover. GeoCarto International 15, 33–38.

Schaefer, G.L., Cosh, M.H., Jackson, T.J., 2007. The USDA natural resources conservation service soil climate analysis network (SCAN). J. Atmos. Ocean. Technol. 24, 2073–2077.

Schoenberg, F.P., Peng, R., Huang, Z., Rundel, P., 2003. Detection of non-linearities in the dependence of burn area on fuel age and climatic variables. Int. J. Wildland Fire 12, 1–6.

Steduto, P., Hsiao, T.C., Raes, D., Fereres, E., 2009. Aquacrop—the FAO crop model to simulate yield response to water: I. Concepts and underlying principles. Agron. J. 101, 426–437.

Stocks, B.J., Lynham, T., Lawson, B., Alexander, M., Wagner, C.V., McAlpine, R., Dube, D., 1989. Canadian forest fire danger rating system: an overview. For. Chron. 65, 258–265.

Torres, R., Snoeij, P., Geudtner, D., Bibby, D., Davidson, M., Attema, E., Potin, P., Rommen, B., Floury, N., Brown, M., et al., 2012. GMES Sentinel-1 mission. Remote Sens. Environ. 120, 9–24.

Van Wagner, C., Forest, P., et al., 1987. Development and structure of the Canadian forest fireweather index system, in: Can. For. Serv., Forestry Tech. Rep, Citeseer.

Vicente-Serrano, S.M., Gouveia, C., Camarero, J.J., Beguería, S., Trigo, R., López-Moreno, J.I., Azorín-Molina, C., Pasho, E., Lorenzo-Lacruz, J., Revuelto, J., et al., 2013. Response of vegetation to drought time-scales across global land biomes. Proc. Natl. Acad. Sci. 110, 52–57.

Wang, X., Xie, H., Guan, H., Zhou, X., 2007. Different responses of MODIS-derived NDVI to root-zone soil moisture in semi-arid and humid regions. J. Hydrol. 340, 12–24.

Weise, D.R., Hartford, R.A., Mahaffey, L., 1998. Assessing live fuel moisture for fire management applications. Assessing Live Fuel Moisture For Fire Management Applications. Pages 49–55 in Teresa L. Pruden and Leonard A. Brennan (eds.).

Westerling, A.L., Hidalgo, H.G., Cayan, D.R., Swetnam, T.W., 2006. Warming and earlier spring increase western US forest wildfire activity. Science 313, 940–943.

Williams, C., McNamara, J., Chandler, D., 2009. Controls on the temporal and spatial variability of soil moisture in a mountainous landscape: the signature of snow and complex terrain. Hydrol. Earth Syst. Sci. 13, 1325–1336.

Wu, D., Zhao, X., Liang, S., Zhou, T., Huang, K., Tang, B., Zhao, W., 2015. Time-lag effects of global vegetation responses to climate change. Glob. Chang. Biol. 21, 3520–3531.

Xia, Y., Mitchell, K., Ek, M., Sheffield, J., Cosgrove, B., Wood, E., Luo, L., Alonge, C., Wei, H., Meng, J., et al., 2012. Continental-scale water and energy flux analysis and validation for the North American Land Data Assimilation System project phase 2 (NLDAS-2): 1. Intercomparison and application of model products. Journal of Geophysical Research: Atmospheres 117.

Yebra, M., Chuvieco, E., Riaño, D., 2008. Estimation of live fuel moisture content from MODIS images for fire risk assessment. Agric. For. Meteorol. 148, 523–536.

Yebra, M., Dennison, P.E., Chuvieco, E., Riano, D., Zylstra, P., Hunt Jr., E.R., Danson, F.M., Qi, Y., Jurdao, S., 2013. A global review of remote sensing of live fuel moisture content for fire danger assessment: moving towards operational products. Remote Sens. Environ. 136, 455–468.

Yebra, M., Quan, X., Riaño, D., Larraondo, P.R., van Dijk, A.I., Cary, G.J., 2018. A fuel moisture content and flammability monitoring methodology for continental Australia based on optical remote sensing. Remote Sens. Environ. 212, 260–272.

Yebra, M., Scortechini, G., Badi, A., Beget, M.E., Boer, M.M., Bradstock, R., Chuvieco, E., Danson, F.M., Dennison, P., de Dios, V.R., et al., 2019. Globe-LFMC, a global plant water status database for vegetation ecophysiology and wildfire applications. Scientific Data 6, 1–8.